Smooth Muscle Cells Orchestrate the Endothelial Cell Response to Flow and Injury

Mercedes Balcells, PhD; Jordi Martorell, MS; Carla Olivé, MS; Marina Santacana, MS; Vipul Chitalia, MD, PhD; Angelo A. Cardoso, MD, PhD; Elazer R. Edelman, MD, PhD

Background—Local modulation of vascular mammalian target of rapamycin (mTOR) signaling reduces smooth muscle cell (SMC) proliferation after endovascular interventions but may be associated with endothelial cell (EC) toxicity. The trilaminate vascular architecture juxtaposes ECs and SMCs to enable complex paracrine coregulation but shields SMCs from flow. We hypothesized that flow differentially affects mTOR signaling in ECs and SMCs and that SMCs regulate mTOR in ECs.

Methods and Results—SMCs and/or ECs were exposed to coronary artery flow in a perfusion bioreactor. We demonstrated by flow cytometry, immunofluorescence, and immunoblotting that EC expression of phospho-S6 ribosomal protein (p-S6RP), a downstream target of mTOR, was doubled by flow. Conversely, S6RP in SMCs was growth factor but not flow responsive, and SMCs eliminated the flow sensitivity of ECs. Temsirolimus, a sirolimus analog, eliminated the effect of growth factor on SMCs and of flow on ECs, reducing p-S6RP below basal levels and inhibiting endothelial recovery. EC p-S6RP expression in stented porcine arteries confirmed our in vitro findings: Phosphorylation was greatest in ECs farthest from intact SMCs in metal stented arteries and altogether absent after sirolimus stent elution.

Conclusions—The mTOR pathway is activated in ECs in response to luminal flow. SMCs inhibit this flow-induced stimulation of endothelial mTOR pathway. Thus, we now define a novel external stimulus regulating phosphorylation of S6RP and another level of EC-SMC crosstalk. These interactions may explain the impact of local antiproliferative delivery that targets SMC proliferation and suggest that future stents integrate design influences on flow and drug effects on their molecular targets. **(*Circulation*. 2010;121:2192-2199.)**

Key Words: blood flow ■ endothelium ■ mammalian target of rapamycin (mTOR) ■ molecular biology ■ muscle, smooth ■ signal transduction ■ stents

Local delivery of antiproliferative drugs limits the intimal hyperplastic response to vascular intervention but may place vessels at risk of thrombosis even late after initial treatment. The intervention, agents used, and means of administration can synergistically induce endothelial dysfunction and delay recovery,[1] leading to impaired vasoreactivity, enhanced platelet aggregation,[2] and elevated tissue factor expression.[3–5] Sirolimus, for example, inhibits smooth muscle cell (SMC) proliferation and intimal hyperplasia after vascular manipulation presumably through effects on signaling within the mammalian target of rapamycin (mTOR) pathway. mTOR is central to the regulation of protein synthesis, ribosomal protein translation, and cap-dependent translation,[6] and its inhibition with sirolimus alters the balance of mTORC1-mTORC2 complexes.[7] Prolonged exposure to sirolimus partially inhibits Akt activation and SMC proliferation.[8] However, sirolimus also induces tissue factor expression[3,4] and dysfunction in endothelial cells (ECs). The impact of flow and drug release on tissue drug distribution and vascular repair has been defined computationally[9–12] and in vivo,[13–15] but the specific flow effects on individual vascular cells have not been fully defined. ECs are especially flow sensitive,[16] and altered hemodynamics may disrupt endothelial health. When ECs become dysfunctional, vascular homeostasis is disrupted, and disease becomes manifest; each element of vascular repair goes awry.[17]

Clinical Perspective on p 2199

We used vessel-like constructs to examine mTOR pathway signaling in isolated ECs, isolated SMCs, and ECs cultured over SMCs. A model system with sequentially layered SMC/EC vessel-like constructs connected to a perfusion bioreactor allowed fine control of hemodynamic parameters,

Received May 4, 2009; accepted February 23, 2010.

From the Harvard–MIT Division of Health Sciences and Technology, Cambridge, Mass (M.B., J.M., C.O., M.S., V.C., E.R.E.); Institut Químic de Sarrià, Ramon Llull University, Barcelona, Spain (M.B., J.M., C.O., M.S.); Boston University School of Medicine, Boston, Mass (V.C.); Indiana University Simon Cancer Center, Indianapolis, Ind (A.A.C.); and Cardiovascular Division, Brigham and Women's Hospital and Harvard Medical School, Boston, Mass (E.R.E.).

Guest Editor for this article was William Wijns, MD.

The online-only Data Supplement is available with this article at http://circ.ahajournals.org/cgi/content/full/CIRCULATIONAHA.109.877282/DC1.

Correspondence to Mercedes Balcells, PhD, MIT, 77 Massachusetts Ave, Cambridge, MA 02139. E-mail merche@mit.edu

Circulation **is available at http://circ.ahajournals.org** **DOI: 10.1161/CIRCULATIONAHA.109.877282**

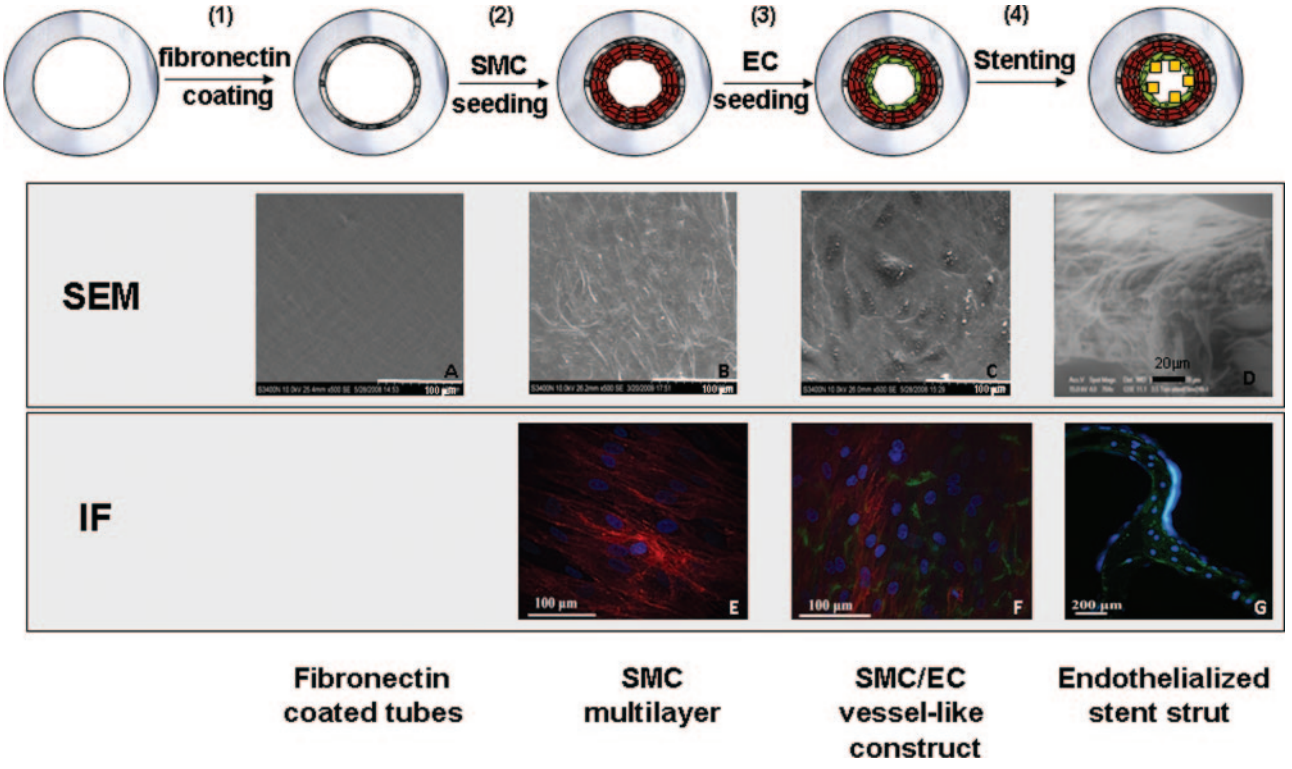

Figure 1. Layer-by-layer assembly and intervention of a vessel-like construct. In vitro model of stent-induced vascular injury. ECs alone or with SMCs were layered onto the inner surface of fibronectin-coated silicon rubber tubes and left intact or stented. Luminal construct morphology at each stage was obtained by scanning electron microscopy (SEM). The cobblestone morphology typical of EC on naïve vessels and in vitro cultures can be observed in the undisturbed SMC/EC vessel-like constructs (C) but is lost on the stent strut surface (D). Immunofluorescence imaging (IF) identified specific cells. ECs (in green) are labeled with anti-CD31 monoclonal antibody conjugated to an Alexa Fluor 488 secondary antibody. SMCs (in red) are labeled with anti–tissue factor monoclonal antibody conjugated to an Alexa Fluor 647 secondary antibody. Each assembly step was imaged in 3 different experiments, each including 3 independent constructs. All constructs were divided into 4 to 6 sections that were scanned and photographed 8 to 10 times.

recapitulating physiological flow. Importantly, these constructs enabled biologically relevant studies of vascular intervention, including bolus drug administration, balloon deployment, and stent implantation. Our data demonstrate a profound difference in EC biology in the presence and absence of SMCs and suggest a far more sophisticated regulatory interaction between alterations in hemodynamics from above and vessel wall from below than classically appreciated.

Methods

Vascular Cell Culture and Bioengineered Vessel-Like Construct

Human coronary artery ECs (Promocell, Heidelberg, Germany) were cultured in EBM-2 basal medium (Lonza, Basel, Switzerland) supplemented with 5% FBS, 1% penicillin-streptomycin, 0.04% hydrocortisone, 0.4% human fibroblast growth factor 2, 0.1% vascular endothelial growth factor, 0.1% R3–insulin-like growth factor-1, 0.1% ascorbic acid, 0.1% human endothelial growth factor, and 0.1% gentamicin-amphotericin 1000 (EC complete medium). Human aortic SMCs (Cambrex, East Rutherford, NJ) were cultured with SmBM-2 basal medium (Lonza) supplemented with 5% CS, 1% glutamine, and 1% penicillin-streptomycin (SMC complete medium). Cells, passages 4 to 6, were fed every 48 hours and incubated at 37°C.

Before cell seeding, 3.18-mm-ID Silastic tubes (Dow Corning, Midland, Mich.) were washed in 0.2% SDS for 20 minutes, rinsed twice with distilled water for 20 minutes, and steam sterilized. Tube length was 12 cm except for experiments with stents, which used 4-cm-long tubes to reduce background signal from undisturbed cells in unstented parts of the tube. Tubes were coated with 100 μg/mL fibronectin (Sigma, St Louis, Mo) in PBS for 2 hours while rotating at 10 rph at 37°C (Figure 1A) and rinsed to remove loosely adsorbed fibronectin. Homotypic constructs were fabricated with injection of ECs or SMCs into fibronectin-coated tubes (8×10^5 cells/mL) and cultured for 24 hours at 37°C under axial rotation. Sequential layering of SMCs, followed by application of ECs, produced SMC/EC vessel-like constructs. SMCs were seeded on fibronectin-coated tubes (8×10^5 cells/mL), forming an SMC multilayer (Figure 1B and 1E). After 24 hours of adhesion under axial rotation, constructs were filled with an EC suspension (8×10^5 cells/mL) and incubated for 24 hours. Cells within constructs were characterized for constitutive and inducible markers and biosecretory function (Table I in the online-only Data Supplement). Appropriate cell assembly within constructs was verified by confocal microscopy, and cell coverage was quantified with MATLAB-based image analysis programs (Video I in the online-only Data Supplement).

The SMC/EC vessel-like constructs were connected to 60-cm-long loops of Silastic tubing containing fresh EC complete medium and rested for 24 hours to ensure complete "endothelialization" (Figure 1C and 1F). Supplemented medium was replaced by EBM-2 medium to starve the cells overnight before perfusion. Cell-seeded constructs were placed in a perfusion bioreactor[18,19] and exposed to controlled coronary artery–like flow: 1-Hz pulsatile flow of 17 dynes/cm^2 average shear stress. In all experiments, samples without flow served as controls. In experiments with growth factors, EC and SMC complete media were used for EC and SMC homotypic constructs, respectively, whereas SMC/EC vessel-like constructs were perfused with EC complete medium.

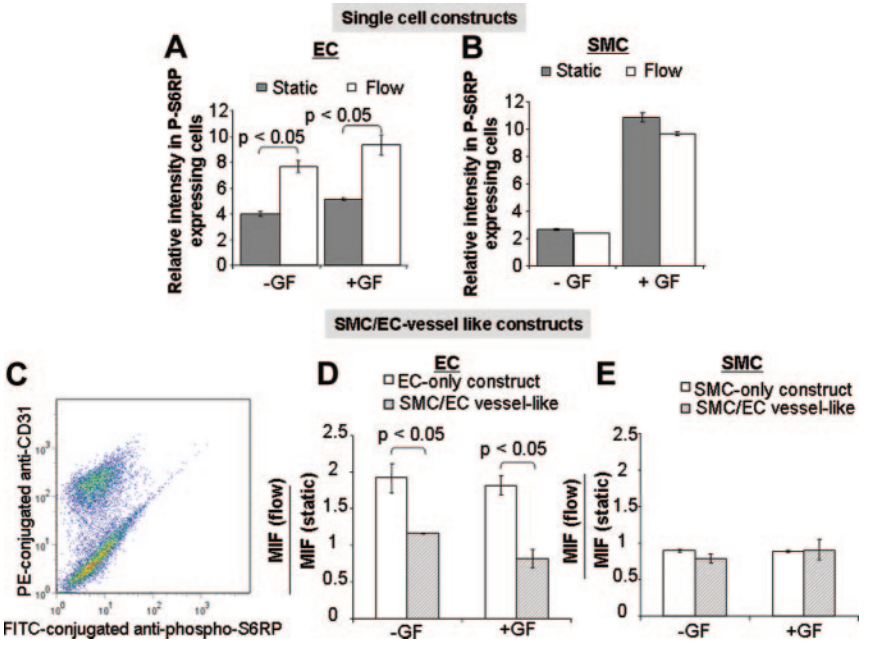

Figure 2. Impact of flow and growth factors on p-S6RP expression. Although coronary artery–like flow upregulated p-S6RP expression in ECs but not in SMCs, growth factor stimulation induced S6RP phosphorylation in SMCs but not ECs (A and B). SMCs regulate EC response to flow. ECs dictate SMC response to growth factors. C, Representative flow cytometric separation of SMCs and ECs in SMC/EC vessel-like constructs. After detachment from tubes, p-S6RP expression in both cell types was quantified with an FITC-conjugated anti–p-S6RP antibody. ECs in the EC/SMC mixture were specifically stained with PE-conjugated CD31 antibody. When ECs were seeded on an SMC multilayer, EC S-6RP phosphorylation became flow independent (D). S-6RP phosphorylation was independent of flow in SMCs both when SMCs were alone and when SMCs were shielded by overlying ECs (E). All figure bars represent the average±SD of 12 data points obtained in 3 experiments that included 4 independent observations of each condition assayed. MIF indicates mean intensity fluorescence.

Injury Model

EC-only and SMC/EC vessel-like constructs were stented with 7-cell stainless steel NIR stents (3.5×16 mm, Medinol, Tel-Aviv, Israel). To discriminate direct drug-mediated effects from flow-mediated modulation of drug treatment, 1 hour before stent implantation, 10 nmol/L temsirolimus (Wyeth, Andover, Mass) was added to the starvation media. This dose abrogates mTOR signaling in ECs.[20] Dimethyl sulfoxide at the doses used has no effect on mTOR activation status.[20]

Measurement of Phosphorylated S6 Ribosomal Protein Expression by Flow Cytometry

We used our perfusion bioreactor and the vessel-like constructs to examine mTOR signaling in cells exposed to coronary-like flow. mTOR activation status was assessed by measurement of phosphorylation levels of S6 ribosomal protein (S6RP), a downstream substrate of TORC1. Phospho-S6RP (p-S6RP) is a more reliable index in our experiments because total mTOR may be conserved even in the face of shunting to the TORC1 or TORC2 protein complexes. ECs in SMC/EC cocultures were identified with PE-conjugated anti-CD31 antibody (BD PharMingen, San Diego, Calif). Double staining of ECs with this antibody and FITC-conjugated anti–p-S6RP allowed cell and signal colocalization. Levels of p-S6RP were measured at "basal" conditions and after flow exposure, stent placement, and incubation with temsirolimus. Cells were recovered from constructs by 3 minutes of trypsin treatment, washed, and resuspended in fixation/permeabilization buffer solution (BD Biosciences, San Jose, Calif) for 30 minutes. Trypsin had no impact on CD31 cytometric detection in ECs. After detachment, samples were rinsed twice with 10% fixation buffer (BD Biosciences) in PBS and incubated in suspension with FITC-conjugated anti–p-S6RP (Cell Signaling Technology, Danvers, Mass) or appropriate isotypic control for 30 minutes at 4°C. Cells were analyzed by flow cytometry with a FACScalibur instrument and CellQuest software (Becton Dickinson, Franklin Lakes, NJ). Positive cells were gated to determine the respective mean intensity fluorescence (Figure 2C); background autofluorescence from unlabeled cells was subtracted; and data were presented as the quotient of mean intensity fluorescence of samples exposed to flow and corresponding static controls.

Radioimmunoprecipitation Assay and Digitonin Extraction

Nonspecific cell lysis was performed by rinsing cell-coated constructs twice with ice-cold PBS and then incubating them for 30 minutes on ice in radioimmunoprecipitation assay buffer containing 50 mmol/L Tris-HCl, pH 7.4, 150 mmol/L NaCl, 1% NP-40, 0.5% sodium deoxycholate, 0.1% SDS, and 5 mmol/L EDTA. The supernatant was obtained after centrifugation for 30 minutes at 4°C. Specific cytosolic extraction of surface cells on the constructs was achieved with digitonin. Cells washed with ice-cold PBS were covered with buffer containing 120 mmol/L KCl, 5 mmol/L KH_2PO_4, 10 mmol/L HEPES, pH 7.4, 2 mmol/L EGTA, and 0.15 mg/mL digitonin (Sigma) and rocked gently on ice for 30 minutes. The gently aspirated supernatant was labeled as digitonin extract.[21,22] The absence of SMCs in the extracts was verified by blotting membranes against anti–SMCα-actin and anti-tubulin antibodies (Sigma; Figure IIA in the online-only Data Supplement).

Western Blot Analysis

We used 10% acrylamide gels (Invitrogen, Carlsbad, Calif) for protein separation. Gels were blotted with Invitrogen gel transfer stacks and blotting system. Membranes were blocked with 5% powdered milk and incubated overnight with primary monoclonal anti–p-S6RP (Cell Signaling; 1:1000 dilution) and anti–β-actin (Santa Cruz Biotechnology, Santa Cruz, Calif; 1:15[thinsp]000 dilution) at 4°C while shaking. After 2 washes with PBS-T (PBS, 0.05% Tween20), membranes were incubated with horseradish peroxidase–conjugated secondary antibodies (Santa Cruz Biotechnology; 1:3500 dilution) for 2 hours while shaking at room temperature. After two 10-minute washes in PBS-T, Supersignal West Femto Maximum Sensitivity Substrate (Pierce Biotechnology Inc, Rockford, Ill) was applied, and luminescence was detected in an Alpha Innotec FluorChem. Densitometry plots were analyzed with ImageJ.

Microscopic Examinations

Endothelial monolayer integrity within constructs was assessed with fluorescence (Perkin-Elmer spinning disk confocal system coupled to a Zeiss Axiovert 200M microscope) and scanning electron microscopy (Figure 1). Constructs, which were embedded in a protective outer tubular layer before removal from the loops to minimize stress and artifactual effects on the cellular lining, were rinsed with PBS and fixed with 4% paraformaldehyde (Mallinckrodt, Hazelwood, Mo) for 20 minutes at room temperature. After 2 consecutive washes with PBS for 10 minutes and 1 hour blotting with 5% goat serum in PBS-BSA (PBS, 1% BSA), ECs and SMCs were labeled for 1 hour with rabbit monoclonal anti-CD31 (Abcam, Cambridge, Mass) and mouse anti–tissue factor (American Diagnos-

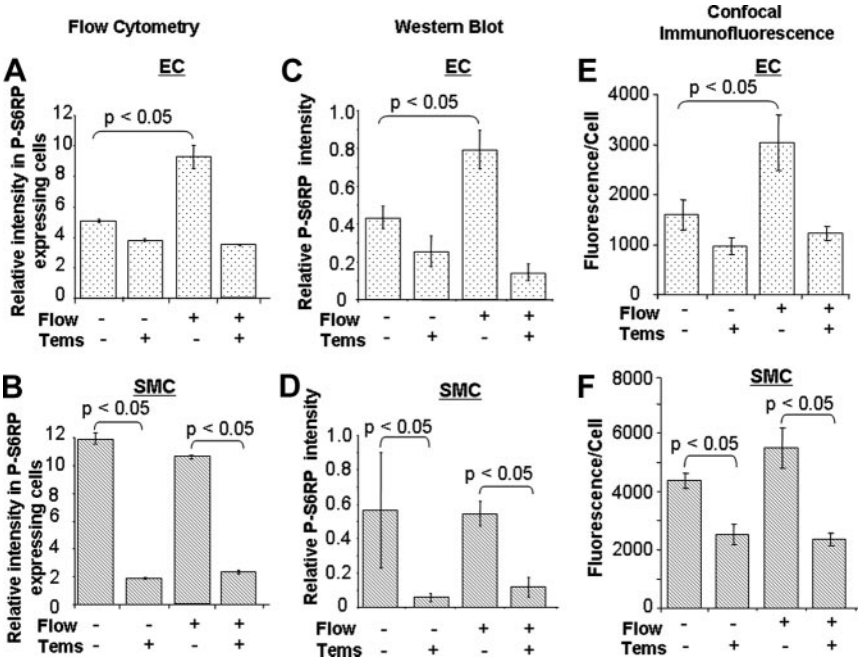

Figure 3. Temsirolimus effectively blocks the mTOR pathway. The flow and temsirolimus response of isolated ECs and SMCs obtained by fluorescence-activated cell sorting (A and B) were confirmed by protein expression by Western blots (C and D) and under confocal immunofluorescence (E and F). n=12 (3 experiments, 4 independent observations of each condition assayed).

tica, Stamford, Conn) diluted 1:50 in PBS-BSA. Cells were rinsed twice with PBS-BSA for 10 minutes and stained with goat anti-rabbit Alexa Fluor 488 and goat antimouse Alexa Fluor 647 (1:100 in PBS-BSA) secondary antibodies and DAPI solution (1:500 in PBS-BSA) for 1 hour. Two 10-minute washes with PBS were performed to remove any unbound antibody. Vessels were sectioned longitudinally with a surgical blade for imaging. To image stents within constructs (Figure 1G), stents were removed from the longitudinally sectioned constructs and cut open with surgical scissors. When p-S6RP expression was imaged (Figure I of the online-only Data Supplement), fixed cells were permeabilized with 0.2% Triton in PBS for 10 minutes. Cells were washed with PBS twice for 10 minutes, blotted, and stained with rabbit monoclonal antibody against p-S6RP (Cell Signaling; 1:50 dilution in PBS-BSA) and the corresponding Alexa Fluor 488–conjugated secondary antibody (1:100 in PBS-BSA).

For scanning electron microscopy, stents were removed from the cell-coated constructs, and stent struts were imaged directly with low-vacuum EI/Philips XL30 FEG environmental scanning electron microscopy (Figure 1D). Cells on constructs were fixed in 4% paraformaldehyde, rinsed with PBS, and subjected to serial dehydration with 30-minute incubations in solutions of increasing ethanol content (50%, 70%, 95%, 100%) and 1-hour incubation in acetone. Specimens were air dried overnight, sputter coated for 45 seconds with a Denton Vacuum Desk II Sputter Coater, and imaged with a Hitachi S-3400N scanning electron microscopy.

In Vivo Studies

The left anterior descending coronary and right coronary arteries of Yucatan pigs were implanted with 6-cell, 3×13-mm bare metal (Neo Stent, Co/Cr alloy) or sirolimus-eluting (Neo Stents coated with 50/50 [wt/wt] polyethylene vinyl acetate and poly-butyl-methacrylate containing 120 μg sirolimus; JnJ/Cordis) stents. Animal care and procedures followed Association for Assessment and Accreditation of Laboratory Animal Care and National Institute of Health (NIH) guidelines. On the 7th (n=3) and 30th (n=8) days after stenting, animals were terminally anesthetized with pentobarbital (65 mg/kg). Then, stented vessels were dissected free and pressure perfused with PBS followed by 10% formalin. After ethanol and xylene processing, vessels were embedded whole in a methyl methacrylate/butyl methacrylate resin (Polysciences Inc, Warrington, Pa) and polymerized under ultraviolet light. Serial cross-sectional planes were obtained along the length of the stents with a precision saw, microtome cut at 5-μm thickness, and stained with ver Hoeff elastin and hematoxylin and eosin stains and for specific cell markers (CD31, α-actin, p-S6RP; Figure III in the online-only Data Supplement). Unstented coronary segments were embedded in paraffin. Rabbit anti–p-S6RP monoclonal antibody (Cell Signaling) with low-temperature antigen retrieval and a tyramide signal amplification system (DakoCytomation) was used for immunohistochemical analysis of mTOR. Quantitative morphometric analysis was performed on the histological sections from each stented artery.

Statistical Analysis

In all figures, data are expressed as average±SD. Nonparametric Kruskal-Wallis test, followed by a Scheffé posthoc analysis of the original measured values normalized to their corresponding controls, was conducted to determine statistical differences between values. Values of $P<0.05$ were considered significant.

Results

Basal mTOR/TORC1 Signaling Is Modulated by Flow in ECs But Not in SMCs

Although ECs and SMCs rendered quiescent by growth factor deprivation exhibited low levels of p-S6RP, they also showed differential responses to flow and growth factor. EC expression of p-S6RP nearly doubled within 20 minutes of exposure to coronary-like flow (1 Hz pulsatile, 17 dynes/cm^2) (1.97±0.2-fold increase; $P<0.5$; Figure 2A). A 1.96±0.4-fold increase in p-S6RP upregulation was confirmed by immunoblotting with Western blotting after whole-cell lysis and with digitonin extraction (Figure 3C and Figure IIB in the online-only Data Supplement). Confocal imaging of adherent ECs revealed 1.91±0.2-fold upregulation of S6RP phosphorylation under flow (Figure 3E and Figure I in the online-only Data Supplement). Growth factor exposure had no significant effect on S6RP phosphorylation in ECs (Figure 2A). In contrast, SMCs were unaffected by flow but exhibited an almost 5-fold increase in p-S6RP expression on growth factor exposure ($P<0.05$ versus static control; Figure 2B). Thus, mTOR/TORC1 signaling in ECs is most sensitive to alter-

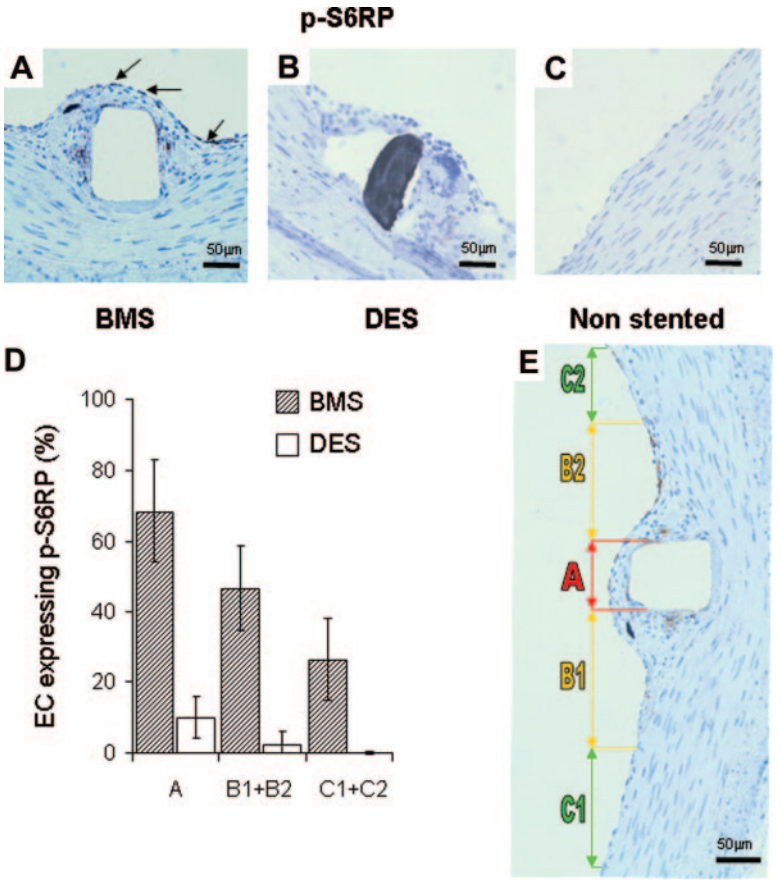

Figure 4. Injury and sirolimus alter p-S6RP expression in ECs. The highest degree of S6RP phosphorylation in vivo occurs when ECs are farthest from intact SMCs. p-S6RP expression was prominent in extracted porcine coronary arteries stented with bare metal stents (BMS) (A; arrows indicate positive staining cells in brown) and eliminated in sirolimus-eluting stents (DES; B). Unstented control arteries (C) had an intact endothelium and media with no detectable p-S6RP staining. The incidence of p-S6RP–positive ECs in the luminal surface correlated with the nature of the underlying layer (D) and is plotted by region relative to the stent strut (E). Region A is directly above the stent strut; B1 and B2 correspond to areas within the neointima adjacent to the stent strut; and C1 and C2 are regions where there is healthy endothelium, no detectable neointima, and viable SMCs within a normal medial layer (E). Only at a distance from the stent strut beyond the neointima/intact media boundary (zones C1 and C2) was the number of p-S6RP–positive ECs significantly reduced. n=12 (3 experiments, 4 independent observations each).

ations in shear stress, whereas the local biochemical milieu dominates in SMCs. Homotypic studies were augmented by SMC/EC vessel-like constructs. Interestingly, the presence of SMC reduced flow-induced S6RP phosphorylation in ECs (mean intensity fluorescence flow/static, 1.16±0.04- versus 1.97±0.2-fold in EC-only vessel-like constructs; $P<0.05$; Figure 2D and Figure IIC in the online-only Data Supplement), and ECs eliminated the growth factor responsiveness of SMC p-S6RP expression (Figure 2E).

Differential Effect of Flow and Static Regimens on p-S6RP Status in ECs After Stent-Induced Injury

Under static conditions, p-S6RP expression in ECs lining conduits rose with stent injury (1.32±0.1-fold) but not when SMCs were also present (0.90±0.2-fold; $P<0.05$). Interestingly, the expected flow-mediated increase in p-S6RP expression seen in quiescent, monolayered ECs was lost in ECs injured by stent placement (0.91±0.1-fold; $P<0.05$ versus static) and reduced when ECs were in SMC/EC vessel-like constructs (0.77±0.1-fold; $P<0.05$ versus static).

mTOR Blockade by Temsirolimus Eliminates In Vitro Flow and Growth Factor–Induced mTOR/TORC1 Activation and Delays Poststenting Re-Endothelization

Sirolimus/FKBP12 complexes interact specifically with mTOR/TORC1, blocking downstream targets, S6K1 and its substrate S6RP. Temsirolimus reduced flow- and growth factor–induced p-S6RP levels in ECs and SMCs (Figure 3). mTOR blockade markedly affected re-endothelialization after stenting. The number of CD31-positive cells on the luminal surface of stents struts after 24 hours of flow exposure was 3.5±0.4-fold ($P<0.05$) reduced by temsirolimus in constructs with ECs alone and by 2.2±0.4-fold ($P<0.05$) with SMCs also present (Figure IV of the online-only Data Supplement). These results confirm that temsirolimus is a powerful blocker of the mTOR machinery and suggest that its effects are more profound when expression of S6RP is highest as in ECs without underlying SMCs.

Immunohistochemical analysis of p-S6RP expression was performed in coronary arteries stented with sirolimus-eluting stents or control bare metal stents. Endothelialization was not significantly different in the different stent arteries (3.1±0.2 versus 2.3±0.50). Specific p-S6RP staining was identified in the endothelium and some leukocytes (macrophages and lymphocytes) in the neointima of the 7-day bare metal stents but no cells stained in the 7-day sirolimus-eluting stent (Figure 4A and 4B). Control unstented arteries did not show any cells expressing p-S6RP (Figure 4C). More important, quantitative analysis of the luminal surface of the bare metal–stented vessels revealed the highest percentage of p-S6RP–positive cells at the neointima luminal surface (Figure 4D and 4E). p-S6RP is upregulated in the neointima of bare metal-stented arteries; phosphorylation inversely correlates with the presence of underlying SMCs. These findings provide in vivo evidence that healthy ECs do not express p-S6RP. Conversely, injured ECs do express p-S6RP, and the expression is sensitive to their

surrounding milieu: fibrin and inflammatory cells in the neointima versus SMCs in the media (Figure III in the online-only Data Supplement). The ability, however, of ECs to restore the balance after intervention is lost in the presence of mTOR inhibitors.

Discussion

The S6/mTOR pathway is critical for vascular reactivity and metabolism. We now show that phosphorylation of S6RP in ECs is flow sensitive and in SMCs is growth factor mediated. We also demonstrate that the response of the intact vessel cannot be appreciated by examination of isolated vascular cells. Using a custom-designed flow system that allowed coating of loop conduits with ECs alone or ECs on layers of SMCs, we demonstrated how EC S6RP signaling is mediated by adjacent SMCs and vice versa. SMCs inhibit flow-mediated mTOR activation in ECs, and reciprocally, ECs regulated the response in SMCs. Cell-seeded perfusion systems allow examination of specific cellular elements under defined flow and shear conditions, with exposure to specific concentrations of vasoregulators and over a short time scale without tissue remodeling. Our vessel-like constructs extend similar systems,[23–30] by introducing a bilayer coculture of ECs and SMCs within tubular structures that enable microscopic examination, programmed chemical and mechanical intervention, correlation of intracellular signaling events with functional outcome, and under static or coronary artery-like flow.[18] The use of cells and defined media here is superior to excised vessels and whole blood because we can associate particular signals with specific cells under precisely controlled flows. Digitonin extraction enables determination of S6RP phosphorylation in ECs even in culture with SMCs. At low concentrations, digitonin, a gentle detergent, selectively punctures 8- to 10-nm holes in the sterol-rich plasma membrane, allowing leakage of cytosolic proteins of up to 200-kDa mass. Moreover, digitonin exerts effects only in cells it directly contacts.[21,22] Digitonin-extracted SMC/EC vessel-like constructs revealed S6RP phosphorylation without effects on SMCs because there was no significant release of SMCα-actin (Figure IIA in the online-only Data Supplement).

The trilaminate architecture of the blood vessel provides structural support and a platform from which to launch an array of intricate paracrine regulation, primary among which are the interactions between ECs and SMCs. Each cell can induce phenotypic transformations and different bioregulatory states in the other.[31,32] ECs spread more slowly and present a less thrombotic phenotype when cultured on SMCs.[33,34] Similarly, the EC procoagulant and proinflammatory phenotype is amplified in coculture with growth factor–stimulated SMCs and subdued in coculture with growth factor–deprived SMCs.[35] In turn, ECs modulate the contractile and growth properties of vascular SMCs.[36–39] Our results concerning flow- and growth factor–mediated activation of S6RP provide further evidence of EC-SMC crosstalk. In health, ECs are exposed to flow and SMCs are buffered from blood by the endothelial monolayer. With injury, the endothelium is disturbed, and SMCs are directly exposed to flow. Classic studies cite these events as critical to mediation of vasomotor tone.[40–42] This view of vascular cell architecture relative to flow perhaps best explains why flow upregulates p-S6RP in ECs and growth factor upregulate this pathway in SMCs. What is fascinating is that this upregulation is observed only for cells in isolation; cocultured cells are far more quiescent. That SMC-EC coregulation extends to p-S6RP is doubly intriguing. The mTOR pathway is a primary metabolic sensor of the cell. SMCs might induce metabolic activity within ECs via a paracrine mechanism or direct cell-cell contact.

Differential expression of proteins within the mTOR signaling pathway has profound implications. Local injury, flow, and chemical inhibition synergize to disrupt the endothelial monolayer, to prevent its restoration, and to impair its function. Interactions between ECs and SMCs are more important in regulating vascular wall hemostasis than previously anticipated; both ECs and SMCs alter the expression of factors in coagulation and fibrinolysis in response to shear stress.[43] Guo and coworkers[44] observed that although laminar shear stress activated AMPK and Akt in ECs, disturbed flow activated only Akt, disrupting the balance of mTOR and S6K and increasing the proportion of ECs in a mitotic state. Our 2-fold upregulation of mTOR in ECs by flow is in direct concert with these studies and has now been expanded to SMCs. Our results indicate that in vessel-like constructs, EC-SMC interaction dominates, altering the dynamics of basal mTOR signaling and overriding growth factor proangiogenic stimulation. Such results take us back to Virchow on the one hand and bring us to the present day of drug-eluting stents and their attendant potential complications on the other. Similar to the triad of Virchow that governs venous thrombosis, we observe that signaling within ECs and SMCs resident in the vessel wall is set by the biochemical milieu established by blood, local flow disruptions, and the state of the wall and its cells. The relative effects of the stent itself on the ECs and SMCs may explain the enhanced sensitivity of the endothelium after local delivery of agents that interfere with mTOR signaling. Endothelial denudation is most prominent between the stent struts at the time of implantation and most rapidly recovers in this region, perhaps because these ECs regenerate over SMCs and can more quickly attain a mature endothelial phenotype. ECs over the stent struts do not readily regain this mature, confluent, and bioregulatory phenotype and retain p-S6RP expression even when physically contiguous because they are distant from SMCs. One might then explain strut-adherent thrombosis in drug-eluting stents with incomplete endothelial healing as evidenced by persistent p-S6RP expression.

The modified triad, inflammation from the foreign materials of the stent, toxic effects of the pooled drug, and flow disruptions from the strut, might contribute to but alone cannot account for the repair in vivo. In vitro stenting results may be masked by surrounding uninjured ECs present in the flow cytometric analysis. Thus, despite the complementary findings that EC-SMC interactions affect EC phosphorylation of S6RP in response to stent injury in vivo and in vitro, the levels of S6RP phosphorylation after stenting in our in vitro system lacked the spatial resolution needed to directly compare them with the in vivo state. Contact-mediated SMC regulation of EC signaling needs to be defined further and

confirmed but may allow better understanding of the vascular response to drug-eluting stents and how drugs that have one putative mode of activity when examined in isolated cultures can behave in unanticipated manners in the intact and injured in vivo system. It is important to remember that stents are placed in diseased arteries with complex bifurcated geometries, blood enriched perhaps in low-density lipoprotein, glucose, and a number of prescription drugs, and plaque. All of those elements will definitively alter the interactions between ECs and SMCs.

The findings that S6RP phosphorylation was flow sensitive in ECs and growth factor sensitive in mural SMCs and that SMCs dominate over ECs have important fundamental and clinical implications. Investigation of the basic signaling should now consider the cells alone and together, and use of drug-eluting stents must integrate stent design influence on flow and drug affect mTOR. The use of flow models, flow-activated cell sorting, intracellular signaling in a coculture of human vascular cells, and modern clinical interventions can provide new insights into fundamental biology. Our flow system can track mTOR and upstream and downstream signaling molecules at rest, under flow, and with exposure to drugs over a span of concentrations and delivery kinetics. Novel endoscopic confocal microscopes allow us to relate flow alterations to cell function and drug localization. Stents are placed in diseased arteries with thickened diseased walls, in the presence of clot and inflammation, with a complex and potentially disarrayed matrix of ECs and SMCs, with complex bifurcated geometries, and with blood enriched with lipoproteins, glucose, and possibly drugs that may be subject to altered flow. All of those elements affect the interactions between ECs and SMCs, and all must be considered in appreciating vascular cell communication and homeostasis, but few of them can be reproduced in a consistent and independent fashion. Flow models with multiple cell systems under defined flow regimens bring us back to Virchow and forward into the era of complex vascular interventions and emerging concepts in vascular biology.

Acknowledgments

We thank Philip Seifert for his support in immunohistochemistry, Sylaja Murikipudi and Laith Rabadi for their support in Western blot analysis, Dr Yoram Richter (Medinol) for the gift of NIR stents, and Wyeth Laboratories for the temsirolimus. We thank Cordis Corp for providing access to specimens used to obtain preclinical in vivo data.

Sources of Funding

This work was supported by NIH/NIGMS RO1/GM049039 (Dr Edelman) and NIH-NIDDK (1K08DK080946; Dr Chitalia). Dr Balcells is supported by the Barcelona Chamber of Commerce and Fundació Empreses IQS.

Disclosures

None.

References

1. Joner M, Finn AV, Farb A, Mont EK, Kolodgie FD, Ladich E, Kutys R, Skorija K, Gold HK, Virmani R. Pathology of drug-eluting stents in humans: delayed healing and late thrombotic risk. *J Am Coll Cardiol*. 2006;48:193–202.
2. Serruys PW, Kukreja N. Late stent thrombosis in drug-eluting stents: return of the "VB syndrome." *Nat Clin Pract Cardiovasc Med*. 2006; 3:637.
3. Steffel J, Latini RA, Akhmedov A, Zimmermann D, Zimmerling P, Luscher TF, Tanner FC. Rapamycin, but not FK-506, increases endothelial tissue factor expression: implications for drug-eluting stent design. *Circulation*. 2005;112:2002–2011.
4. Camici GG, Steffel J, Amanovic I, Breitenstein A, Baldinger J, Keller S, Luscher TF, Tanner FC. Rapamycin promotes arterial thrombosis in vivo: implications for everolimus and zotarolimus eluting stents. *Eur Heart J*. 2010;31:236–242.
5. Smith EJ, Jain AK, Rothman MT. New developments in coronary stent technology. *J Interv Cardiol*. 2006;19:493–499.
6. Jiang BH, Liu LZ. Role of mTOR in anticancer drug resistance: perspectives for improved drug treatment. *Drug Resist Updat*. 2008;11: 63–76.
7. Zeng Z, Sarbassov dos D, Samudio IJ, Yee KW, Munsell MF, Ellen Jackson C, Giles FJ, Sabatini DM, Andreeff M, Konopleva M. Rapamycin derivatives reduce mTORC2 signaling and inhibit AKT activation in AML. *Blood*. 2007;109:3509–3512.
8. Sarbassov DD, Ali SM, Sengupta S, Sheen JH, Hsu PP, Bagley AF, Markhard AL, Sabatini DM. Prolonged rapamycin treatment inhibits mTORC2 assembly and Akt/PKB. *Mol Cell*. 2006;22:159–168.
9. Kolachalama VB, Tzafriri AR, Arifin DY, Edelman ER. Luminal flow patterns dictate arterial drug deposition in stent-based delivery. *J Control Release*. 2009;133:24–30.
10. Balakrishnan B, Dooley J, Kopia G, Edelman ER. Thrombus causes fluctuations in arterial drug delivery from intravascular stents. *J Control Release*. 2008;131:173–180.
11. Balakrishnan B, Dooley JF, Kopia G, Edelman ER. Intravascular drug release kinetics dictate arterial drug deposition, retention, and distribution. *J Control Release*. 2007;123:100–108.
12. Balakrishnan B, Tzafriri AR, Seifert P, Groothuis A, Rogers C, Edelman ER. Strut position, blood flow, and drug deposition: implications for single and overlapping drug-eluting stents. *Circulation*. 2005;111: 2958–2965.
13. Miyauchi K, Kasai T, Yokayama T, Aihara K, Kurata T, Kajimoto K, Okazaki S, Ishiyama H, Daida H. Effectiveness of statin-eluting stent on early inflammatory response and neointimal thickness in a porcine coronary model. *Circ J*. 2008;72:832–838.
14. Baker AB, Groothuis A, Jonas M, Ettenson DS, Shazly T, Zcharia E, Vlodavsky I, Seifert P, Edelman ER. Heparanase alters arterial structure, mechanics, and repair following endovascular stenting in mice. *Circ Res*. 2009;104:380–387.
15. Jonas M, Edelman ER, Groothuis A, Baker AB, Seifert P, Rogers C. Vascular neointimal formation and signaling pathway activation in response to stent injury in insulin-resistant and diabetic animals. *Circ Res*. 2005;97:725–733.
16. Blackman BR, Garcia-Cardena G, Gimbrone MA Jr. A new in vitro model to evaluate differential responses of endothelial cells to simulated arterial shear stress waveforms. *J Biomech Eng*. 2002;124:397–407.
17. Garcia-Cardena G, Gimbrone MA Jr. Biomechanical modulation of endothelial phenotype: implications for health and disease. *Handb Exp Pharmacol.* 2006;79–95.
18. Balcells M, Fernandez Suarez M, Vazquez M, Edelman ER. Cells in fluidic environments are sensitive to flow frequency. *J Cell Physiol*. 2005;204:329–335.
19. Methe H, Balcells M, Alegret Mdel C, Santacana M, Molins B, Hamik A, Jain MK, Edelman ER. Vascular bed origin dictates flow pattern regulation of endothelial adhesion molecule expression. *Am J Physiol Heart Circ Physiol*. 2007;292:H2167–H2175.
20. Costa LF, Balcells M, Edelman ER, Nadler LM, Cardoso AA. Proangiogenic stimulation of bone marrow endothelium engages mTOR and is inhibited by simultaneous blockade of mTOR and NF-kappaB. *Blood*. 2006;107:285–292.
21. Chitalia VC, Foy RL, Bachschmid MM, Zeng L, Panchenko MV, Zhou MI, Bharti A, Seldin DC, Lecker SH, Dominguez I, Cohen HT. Jade-1 inhibits Wnt signalling by ubiquitylating beta-catenin and mediates Wnt pathway inhibition by pVHL. *Nat Cell Biol*. 2008;10:1208–1216.
22. Schulz I. Permeabilizing cells: some methods and applications for the study of intracellular processes. *Methods Enzymol*. 1990;192:280–300.
23. Niwa K, Kado T, Sakai J, Karino T. The effects of a shear flow on the uptake of LDL and acetylated LDL by an EC monoculture and an EC-SMC coculture. *Ann Biomed Eng*. 2004;32:537–543.

24. Wada Y, Sugiyama A, Kohro T, Kobayashi M, Takeya M, Naito M, Kodama T. In vitro model of atherosclerosis using coculture of arterial wall cells and macrophage. *Yonsei Med J*. 2000;41:740–755.
25. Chiu JJ, Chen LJ, Lee PL, Lee CI, Lo LW, Usami S, Chien S. Shear stress inhibits adhesion molecule expression in vascular endothelial cells induced by coculture with smooth muscle cells. *Blood*. 2003;101:2667–2674.
26. Chiu JJ, Chen LJ, Chen CN, Lee PL, Lee CI. A model for studying the effect of shear stress on interactions between vascular endothelial cells and smooth muscle cells. *J Biomech*. 2004;37:531–539.
27. Fillinger MF, Sampson LN, Cronenwett JL, Powell RJ, Wagner RJ. Coculture of endothelial cells and smooth muscle cells in bilayer and conditioned media models. *J Surg Res*. 1997;67:169–178.
28. Nackman GB, Bech FR, Fillinger MF, Wagner RJ, Cronenwett JL. Endothelial cells modulate smooth muscle cell morphology by inhibition of transforming growth factor-beta 1 activation. *Surgery*. 1996;120: 418–425.
29. Jacot JG, Wong JY. Endothelial injury induces vascular smooth muscle cell proliferation in highly localized regions of a direct contact co-culture system. *Cell Biochem Biophys*. 2008;52:37–46.
30. Gong Z, Niklason LE. Blood vessels engineered from human cells. *Trends Cardiovasc Med*. 2006;16:153–156.
31. Xu S, He Y, Vokurkova M, Touyz RM. Endothelial cells negatively modulate reactive oxygen species generation in vascular smooth muscle cells: role of thioredoxin. *Hypertension*. 2009;54:427–433.
32. Wang YH, Yan ZQ, Shen BR, Zhang L, Zhang P, Jiang ZL. Vascular smooth muscle cells promote endothelial cell adhesion via microtubule dynamics and activation of paxillin and the extracellular signal-regulated kinase (ERK) pathway in a co-culture system. *Eur J Cell Biol*. 2009;88:701–709.
33. Wallace CS, Strike SA, Truskey GA. Smooth muscle cell rigidity and extracellular matrix organization influence endothelial cell spreading and adhesion formation in coculture. *Am J Physiol Heart Circ Physiol*. 2007; 293:H1978–H1986.
34. Imberti B, Seliktar D, Nerem RM, Remuzzi A. The response of endothelial cells to fluid shear stress using a co-culture model of the arterial wall. *Endothelium*. 2002;9:11–23.
35. Rose SL, Babensee JE. Smooth muscle cell phenotype alters cocultured endothelial cell response to biomaterial-pretreated leukocytes. *J Biomed Mater Res A*. 2008;84:661–671.
36. Mosse PR, Campbell GR, Campbell JH. Smooth muscle phenotypic expression in human carotid arteries, II: atherosclerosis-free diffuse intimal thickenings compared with the media. *Arteriosclerosis*. 1986;6:664–669.
37. Herman IM, Castellot JJ Jr. Regulation of vascular smooth muscle cell growth by endothelial-synthesized extracellular matrices. *Arteriosclerosis*. 1987;7:463–469.
38. Sabatini PJ, Zhang M, Silverman-Gavrila R, Bendeck MP, Langille BL. Homotypic and endothelial cell adhesions via N-cadherin determine polarity and regulate migration of vascular smooth muscle cells. *Circ Res*. 2008;103:405–412.
39. Mack PJ, Zhang Y, Chung S, Vickerman V, Kamm RD, Garcia-Cardena G. Biomechanical regulation of endothelial-dependent events critical for adaptive remodeling. *J Biol Chem*. 2009;284:8421–8420.
40. Feletou M, Vanhoutte PM. Endothelium-derived hyperpolarizing factor: where are we now? *Arterioscler Thromb Vasc Biol*. 2006;26:1215–1225.
41. Furchgott RF. Nitric oxide: from basic research on isolated blood vessels to clinical relevance in diabetes. *An R Acad Nac Med (Madr)*. 1998;115: 317–331.
42. Furchgott RF. Endothelium-derived relaxing factor: discovery, early studies, and identification as nitric oxide. *Biosci Rep*. 1999;19:235–251.
43. Helenius G, Hagvall SH, Esguerra M, Fink H, Soderberg R, Risberg B. Effect of shear stress on the expression of coagulation and fibrinolytic factors in both smooth muscle and endothelial cells in a co-culture model. *Eur Surg Res*. 2008;40:325–332.
44. Guo D, Chien S, Shyy JY. Regulation of endothelial cell cycle by laminar versus oscillatory flow: distinct modes of interactions of AMP-activated protein kinase and Akt pathways. *Circ Res*. 2007;100:564–571.

CLINICAL PERSPECTIVE

Local delivery of antiproliferative drugs limits restenosis but may increase thrombosis even late after intervention. Device implantation and drug administration can synergistically induce endothelial dysfunction and delay recovery, impairing vasoreactivity, enhancing platelet aggregation, and elevating tissue factor expression. As stents are placed in increasingly complex geometries in the face of local and systemic disease, in the presence of clot and inflammation, a complex spectrum of issues must be considered that can no longer be intuited or dissected from in vivo experiments. We developed a model flow system examining signaling in vascular cells under controlled physiological flows. Our data demonstrate a profound difference in endothelial cell biology in the presence and absence of smooth muscle cells and suggest a far more sophisticated regulatory interaction between alterations in hemodynamics from above and vessel wall from below than classically appreciated. Similar to the triad that governs venous thrombosis, we now observe that signaling within vascular endothelial and smooth muscle cells is set by the biochemical milieu established by blood, local flow disruptions, and the state of the wall and its cells. The relative effects of the stent itself on the cells may explain the enhanced sensitivity of the endothelium after local delivery of agents that interfere with mammalian target of rapamycin signaling, placing vessels at risk of thrombosis even late after the initial treatment. Flow models with multiple cell systems bring us back to Virchow and forward into the era of complex vascular interventions and emerging concepts in vascular biology.